Pergamon

Int. J. Mech. Sci. Vol. 40, No. 10, pp. 977–988, 1998

Printed in Great Britain
0020–7403/98 $19.00 + 0.00

PII: S0020–7403(97)00141–0

CONTACT PROBLEMS FOR A WEDGE WITH ROUNDED APEX

M. CIAVARELLA*, D. A. HILLS†‡ and G. MONNO*

*Dipartimento di Progettazione e Produzione Industriale, Politecnico di Bari, Viale Japigia 182, Bari, Italy; and ‡Department of Engineering Science, Oxford University, Oxford OX1 3PJ, U.K.

(*Received* 7 *February* 1997; *and in revised form* 31 *July* 1997)

Abstract—Elastic contact between a shallow elastic wedge, whose apex is blunted by a finite radius, and an elastically similar half-plane is studied. A closed-form contact law is found, and the interior stress field is then deduced using a Muskhelishvili's solution in series form, for frictionless and sliding conditions. This geometry removes one of the principal objections to classical solutions to the wedge indentation problem—the unrealistic infinite stress concentration implied by an atomically sharp apex—and in the latter part of the paper the strength of the contact is evaluated explicitly. Further, cases of partial slip associated with the application of tangential load less than needed to cause sliding are considered. © 1998 Elsevier Science Ltd. All rights reserved

Keywords: contact stresses, fretting fatigue pads, asperity contacts.

1. INTRODUCTION

Classical elastic contact problems for the wedge and cone are attractive analytically because they have a relatively simple form of solution for the contact law, and the interior state of stress induced may also be found easily,* including the effects of sliding frictional shear tractions [1]. However, results for these geometries are less useful when applied to real problems because the state of stress at the apex of the indenter is singular, so that the implied strength of the contact is zero. In practice, the singular state of stress would not exist, partly because there will be a finite curvature at the apex, and partly because the singular state of stress would be relieved by local plastic flow. The principal applications of this geometry are to an understanding of the stress state induced beneath asperities on rough surfaces [2], the contacts arising in certain fretting fatigue experiments [3], the loading imposed by stylus instruments such as surface profilometers, and, more qualitatively, to some types of elastic indentation testing of brittle materials. In particular, the use of indenters having a linear profile is attractive for fretting fatigue experiments as this permits a wide range of size of *incomplete contacts* to be obtained, thus facilitating a control of the "size effect", i.e. the different fretting fatigue behavior of the material under geometrically identical contacts of varying *size*.

It is the intention in the present paper to remove the idealization that the indenter apex is perfectly sharp, and to replace it with a circular arc, idealized, in the spirit of the Hertzian contact, by a parabola. The geometry is shown in Fig. 1, and it will be appreciated that, if the overall width of the contact, b, is less than or equal to the extent of the curved portion of the tip, a, the Hertzian solution must be recovered, whilst as the ratio a/b becomes very small the effect of the curvature will become negligible and the wedge solution should result. For intermediate cases the use of a little-known approach due to Shtayerman [4] provides the solution, which will first be discussed. The interior stress field will then be deduced, using a Muskhelishvili potential procedure, and these results will be used to judge the strength of the contact based on first yield and maximum tension.

2. FORMULATION

The geometry examined is shown in Fig. 1 and the problem is formulated for either a rigid punch, or an elastic punch which may be approximated as a half-plane, i.e. with small exterior angle, θ, of

†Author to whom all correspondence should be addressed.

*The interior stress field in the case of the sharp wedge has also been found from a series representation of the Muskhelishvili's potential [1]. However, fewer terms in the series are needed in the present form of the solution for the rounded wedge to achieve a comparable accuracy.

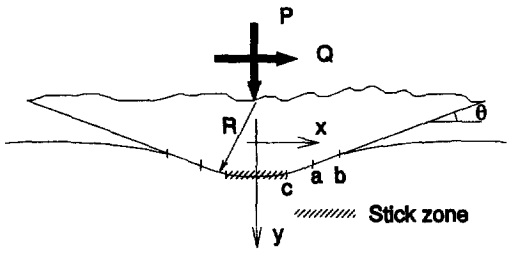

Fig. 1. Geometry of the problem.

the wedge. This is not usually restrictive, since only punches of this kind are of practical interest for fretting fatigue studies, whereas pointed indenters like those used in hardness testing (Vickers, etc.) would induce a α-power singularity in the elastic regime, and require an elasticity treatment appropriate to the elastic wedge. Moreover, in the rounded tip case, the half-plane hypothesis is *more* justifiable, since the contact starts as a Hertzian one, where the validity of the half-plane approximation has already been verified, and approaches the wedge case only in the limit when the rounded part becomes a negligible part of the contact. The well-established technique of integral equations for half-planes may therefore be used, as developed by Shtayerman [4] and Muskhelishvili [5], and reported in Hills *et al.* [6]. Both indenter and half-plane may have finite and different elastic constants, but the solution to be developed is precise only when either (a) there are no shearing tractions present, which in turn requires the coefficient of interfacial friction, f, to vanish, or (b) the materials are elastically similar. If neither of these conditions holds there will be a small surface normal relative displacement induced by the shearing tractions, which will, in turn, modify the pressure distribution, but experience with related geometries has shown this effect to be small [7].

The normal traction distribution over the contact is given by the solution of the following integral equation [6, f.2.17 p. 51], over the contact region L:

$$\frac{1}{A}h'(x) = \frac{1}{\pi}\int_L \frac{p(\xi)\mathrm{d}\xi}{x-\xi}, \tag{1}$$

where A is a measure of the composite compliance of the bodies, defined under plane strain conditions by

$$A = \frac{2}{E_1}(1-\nu_1^2) + \frac{2}{E_2}(1-\nu_2^2), \tag{2}$$

in which E_i is the Young's modulus and ν_i is the Poisson's ratio of body i.

Here both $p(b)$ and $p(-b)$ are bounded (the so-called *incomplete contact conditions*), and it may be proved that $p(\pm b) = 0$ must hold,† which means that the general solution for a contact over the range $-b \leqslant x \leqslant b$ is [4]

$$p(x) = \frac{1}{\pi A}\sqrt{b^2-x^2}\int_{-b}^{b}\frac{h'(t)}{\sqrt{b^2-t^2}(t-x)}\,\mathrm{d}t. \tag{3}$$

The function $h(x)$ is the amount of overlap if the bodies could freely interpenetrate each other, and is therefore defined, if rigid-body rotation is constrained, from the geometry of the undeformed bodies $y = f_1(x)$ and $y = f_2(x)$ as

$$h(x) = C - [f_1(x) - f_2(x)], \tag{4}$$

where C is the rigid body motion to bring the two bodies into contact. Equilibrium between the applied load and the pressure distribution requires that

$$P = -\int_{-b}^{b} p(x)\,\mathrm{d}x = -\frac{1}{A}\int_{-b}^{b}\frac{h'(t)t\,\mathrm{d}t}{\sqrt{b^2-t^2}}. \tag{5}$$

†Under the Lipschitz continuity condition for the function profile.

In the case under consideration, the geometry is such that

$$h'(x) = \begin{cases} \theta, & -b \leqslant x \leqslant -a, \\ -\theta(x/a), & -a \leqslant x \leqslant +a, \\ -\theta, & +a \leqslant x \leqslant +b, \end{cases} \tag{6}$$

where θ is the external angle of the wedge (Fig. 1) which must remain small if the indenter is to be given a finite compliance; (a) to maintain the realism of the half-plane idealization, and (b) for the strains in the vicinity of the apex to be within the definition of linear elasticity theory, for cases where $a/b \ll 1$. From basic geometric considerations, the radius of the rounded tip is $R \simeq a/\theta$.

3. CONTACT LAWS

3.1. *Frictionless normal indentation*

Carrying out the integration of Eqns (3) and (5) (see the Appendix for details), it may be shown that the solution is given by

$$\frac{AP}{\theta} = \frac{a}{\sin^2 \varphi_0}\left(\frac{\sin 2\varphi_0}{2} + \varphi_0\right), \tag{7}$$

$$\frac{\pi A}{\theta} p(\varphi) = \ln\left|\tan\frac{\varphi + \varphi_0}{2}\tan\frac{\varphi - \varphi_0}{2}\right| - 2\varphi_0\frac{\cos\varphi}{\sin\varphi_0} - \frac{\sin\varphi}{\sin\varphi_0}\ln\left|\frac{\sin(\varphi - \varphi_0)}{\sin(\varphi + \varphi_0)}\right|, \tag{8}$$

where

$$\varphi = \arcsin\frac{x}{b}.$$

Considering a as a given geometrical quantity, Eqn (7) determines the dimension b of the contact area, through the auxiliary angle φ_0 (where $\varphi_0 = \arcsin a/b$), as a function of the load, and Eqn (8) gives the pressure distribution in the region $-\pi/2 \leqslant \varphi \leqslant \pi/2$, which corresponds to the physical region $-b \leqslant x \leqslant b$, as $x = a\sin\varphi/\sin\varphi_0$. In particular, the pressure at the straight/rounded part transition point is clearly finite, and is given by

$$\frac{\pi A}{\theta} p(\varphi_0) = \ln\left|\frac{1}{2}\tan\varphi_0 \sin 2\varphi_0\right| - 2\frac{\varphi_0}{\tan\varphi_0}, \tag{9}$$

whilst the maximum pressure, at the centre of the contact area, is

$$\frac{\pi A}{\theta} p(0) = 2\left[\ln\left(\tan\frac{\varphi_0}{2}\right) - \frac{\varphi_0}{\sin\varphi_0}\right]. \tag{10}$$

It may be observed that the equation relating the contact area dimension with the applied load is not only non-linear, but transcendental. However, with a modern software system, this is in fact a minor drawback compared with solutions to the single-function profile case. It may be seen from Eqn (8) that as $a/b \to 1$ the classical Hertzian pressure distribution (for a *parabolic* punch on the half-plane) is recovered, since $\varphi_0 = \pi/2$ and $k = 1/R = \theta/a$ is the curvature of the punch, giving the following well-known results ($x = a\sin\varphi$):

$$\frac{AP}{k} = \frac{\pi}{2}a^2, \tag{11}$$

$$p(\varphi) = -\frac{2P}{\pi a}\cos\varphi = -\frac{2P}{\pi a^2}\sqrt{a^2 - x^2}. \tag{12}$$

On the other hand, as $a/b \to 0$, the standard wedge solution is recovered, as $\varphi_0 \to 0$, $x = b\sin\varphi$, and

$$\frac{AP}{\theta} = 2b, \tag{13}$$

$$p(\varphi) = \frac{P}{\pi b}\ln\left|\tan\frac{\varphi}{2}\right| = -\frac{P}{\pi b}\cosh^{-1}\left|\frac{b}{x}\right|. \tag{14}$$

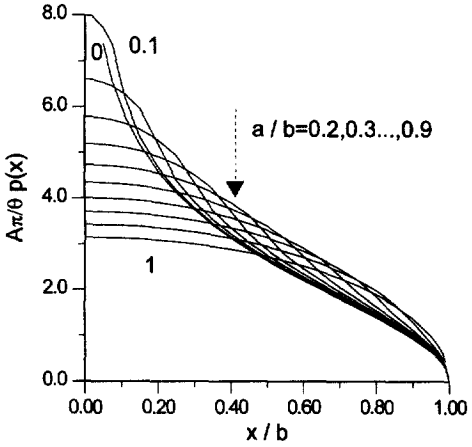

Fig. 2. Non-dimensionalized contact pressures $-p(x/b)A\pi/\theta$ for ratios $a/b = 0.1, 0.1, \ldots, 1$. The sharp wedge singular solution is obtained for $a/b = 0$, the Hertzian solution for $a/b = 1$.

Figure 2 displays the normalized contact pressure distribution found for intermediate cases. It may be noted that the case $a/b = 0.1$ is practically coincident with the limiting sharp wedge case, apart from the region $|x/b| < 0.2$.

3.1.1. *Small rounded tip.* Even simpler results can be obtained in the case where the rounded tip is small, i.e. $a/b \to 0$, which is of practical relevance for engineering design, particularly of styli. As this limit is approached $\varphi_0 = \arcsin a/b \approx a/b$, and the relation between load and contact area is given, to a first-order approximation, by the same linear relation as the case of a sharp wedge, i.e.

$$\frac{AP}{\theta} = 2b, \tag{15}$$

whilst the maximum pressure remains finite and is given by

$$\frac{\pi A}{\theta} p(0) = 2\left[\ln\left(\frac{a}{2b}\right) - 1\right], \tag{16}$$

which goes logarithmically to infinity as the rounded part becomes perfectly sharp.

3.2. *Sliding and partial slip*

Provided the contact is uncoupled, that is the contacting bodies are elastically similar (Dundurs' constant $\beta = 0$), full sliding conditions will occur if the tangential load reaches the limit $|Q| = fP$, and the shear tractions will simply be given by $|q(x)| = -fp(x)$. More interesting is the case of partial slip, i.e. when $|Q| \leqslant fP$ and $|Q|$ is increased monotonically from zero. This problem requires the use of a second integral equation, that relates the surface shearing tractions $q(x)$ to the displacement of particles parallel with the surface. It is [6, f.2.22 p. 53], again for the case of elastically similar materials

$$\frac{1}{A} g'(x) = \frac{1}{\pi} \int_L \frac{q(\xi)\,\mathrm{d}\xi}{x - \xi}, \tag{17}$$

where $g(x)$ is the relative tangential displacement of surface particles, and $g'(x) = \mathrm{d}g(x)/\mathrm{d}x$ is its derivative. As we are considering the case when Dundurs' constant (β) vanishes, Eqn (17) and its counterpart for the normal pressure (1) are uncoupled, and the eccentricity of the stick zone has to be zero. Further, upon applying a normal load, P, alone, there is no tendency for surface particles to slip, and hence the initial stick zone envelopes the entire contact. The pressure will be given *exactly* by the frictionless solution. A partial slip regime will arise as a monotonically increasing tangential force, Q, less than the value needed to produce full slip of the indenter on the half-plane, i.e. $|Q| < fP$, is applied.

Within the stick zone the relative tangential displacement of surface particles must be zero, as for elastically similar materials there is no relative tangential displacement during the normal loading, so that [6, f.4.2 p. 109]‡

$$g'(x) = 0, \quad -c < x < c \tag{18}$$

and the shearing traction must be less than the limiting value, i.e. [6, f.4.3 p. 110]

$$|q(x)| < -fp(x), \quad -c < x < c. \tag{19}$$

Here, c is the half-width of the stick zone. Further, within the slip zones the shearing traction is limited by friction, so that [6, f.4.4 p. 110]

$$|q(x)| = -fp(x) \quad \begin{cases} -b < x < -c \\ +c < x < +b \end{cases} \tag{20}$$

and the shear traction must always oppose the direction of relative change in the direction of slip for a quasi-static contact [6, f.4.5 p. 110],

$$\operatorname{sgn}(q(x)) = sgn\left(\frac{\partial g}{\partial t}\right), \quad -c < x < c. \tag{21}$$

A monotonically increasing shearing force, Q, will therefore give rise to advancing slip, and under these circumstances, Eqn (21) is automatically satisfied.

We will consider $q(x) = fp(x) + q^*(x)$, i.e. the shear tractions arising in the contact as a superposition of the full sliding case, and a perturbation, $q^*(x)$. We need to consider two cases, viz., when the dimension of the stick zone, c, is less than the dimension of rounded part of the indenter $c < a$, and the case when the edge of the stick zone lies in the linear part of the indenter profile $c > a$.

In the first case $0 < c < a$, the integral equation for behavior in the tangential direction [Eqns (17) and (19)] states that in the stick zone the following integral relation holds:

$$0 = \frac{1}{\pi}\int_{-b}^{b} \frac{q(\xi)\,d\xi}{x-\xi} = -f\frac{k}{A}x + \frac{1}{\pi}\int_{-c}^{c} \frac{q^*(\xi)\,d\xi}{x-\xi}, \quad |x| < c \tag{22}$$

as the integral of the full sliding term ($fp(x)$) can be simplified according to Eqn (1). Since only bounded solutions can be considered for $q^*(x)$, and this quantity has to be zero in the regions $c < |x| < b$, Eqn (22) is a standard Cauchy integral equation which may be inverted. It transpires that $q^*(\xi)$ has the Cattaneo–Mindlin shape for a parabolic punch, i.e.

$$q^*(x) = f\frac{k}{A}\sqrt{c^2 - x^2}. \tag{23}$$

This result holds whether $b < a$ (the standard Hertz case, and we expect to recover the Mindlin solution), or $b > a$, where the pressure present on the straight part of the indenter has an influence. The dimension of the stick zone is obtained from the equation for tangential equilibrium.

Turning to the case $c > a$, we have, for $|x| < c$,

$$0 = \frac{1}{\pi}\int_{L} \frac{q(\xi)\,d\xi}{x-\xi} = \frac{f}{A}h'(x) + \frac{1}{\pi}\int_{-c}^{c} \frac{q^*(\xi)\,d\xi}{x-\xi},$$

$$\frac{1}{\pi}\int_{-c}^{c} \frac{-q^*(\xi)/f\,d\xi}{x-\xi} = \frac{1}{A}\begin{cases} \theta, & -c \leqslant x \leqslant -a, \\ -\theta(x/a), & -a \leqslant x \leqslant +a, \\ -\theta, & +a \leqslant x \leqslant +c, \end{cases} \tag{24}$$

as again, from Eqn (1) for normal surface displacements, the transform of the contact pressure is equal to the profile derivative. This equation is of the same form as that for the pressure, and can be solved analytically, as can the equation for tangential equilibrium, by the same method as that described above. Giving only the result, it may be shown that, defining $\omega_0 = \arcsin a/c$, and mapping

‡Apart from the case where a uniform strain is applied to the specimen as a bulk stress.

the region $-c \leqslant x \leqslant c$ by means of the relation $x = a(\sin\omega/\sin\omega_0)$, one has

$$\frac{AQ^*}{\theta f} = \frac{a}{\sin^2\omega_0}\left(\frac{\sin 2\omega_0}{2} + \omega_0\right), \tag{25}$$

and

$$-\frac{\pi A}{\theta} q^*(\omega)/f = \ln\left|\tan\frac{\omega+\omega_0}{2}\tan\frac{\omega-\omega_0}{2}\right| - 2\omega_0\frac{\cos\omega}{\sin\omega_0} - \frac{\sin\omega}{\sin\omega_0}\ln\left|\frac{\sin(\omega-\omega_0)}{\sin(\omega+\omega_0)}\right| \tag{26}$$

Equation (25) determines the angle ω_0, and so implicitly gives the size of the stick zone as a function of the corrective tangential load Q^*, after which Eqn (26) gives the shear in the region $-\pi/2 \leqslant \varphi \leqslant \pi/2$, which corresponds to the region $-c \leqslant x = a(\sin\omega/\sin\omega_0) \leqslant c$. In particular, the corrective shear stress at the straight/rounded transition point is finite, as two logarithmic terms cancel each other, i.e.

$$-\frac{\pi A}{\theta} q^*(\omega_0)/f = \ln\left|\frac{1}{2}\tan\omega_0\sin 2\omega_0\right| - 2\frac{\omega_0}{\tan\omega_0},$$

whilst the maximum corrective shear traction, at the centre of the contact area, is

$$-\frac{\pi A}{\theta} q^*(0)/f = 2\left[\ln\left(\tan\frac{\omega_0}{2}\right) - \frac{\omega_0}{\sin\omega_0}\right]. \tag{27}$$

The solution on the unloading case, as well as more general oscillating loadings, can equally be obtained by a similar procedure, but is omitted for brevity.

4. INTERIOR STRESS FIELD

Whilst a knowledge of the contact law is important, it is the complete interior stress field which is needed in other to assess fully the implications of the wedge apex radius. Muskhelishvili's approach is eminently suitable for half-plane problems, and as it is very straightforward to include the effects of sliding friction this will be done for generality. However, the provisos made in the formulation section must be borne in mind; the solution deduced above will only be precisely true for a *sliding* indenter if the wedge and half-plane are elastically similar, or more precisely, if Dundurs' second constant for the pair vanishes.

As the shear traction, $q(x) = fp(x)$ throughout the whole contact, Muskhelishvili's potential is given by

$$\Phi(z) = \frac{1-\mathrm{i}f}{2\pi\mathrm{i}}\int_{-1}^{1}\frac{p(t)}{t-z}\,\mathrm{d}t, \tag{28}$$

where dimensionless coordinates are now adopted for x, y, t, $z = x + \mathrm{i}y$, by normalizing them with respect to the contact half-width b, and $p(x)$ is expanded in terms of Chebyshev polynomials $U_{2n}(x)$ as[§]

$$p(x) = -\sqrt{1-x^2}\sum_{n=0}^{\infty} b_n U_{2n}(x). \tag{29}$$

The corresponding Muskhelishvili's potential is [6]

$$\Phi(z) = \frac{1-\mathrm{i}f}{2\pi\mathrm{i}}\int_{-1}^{1}\frac{p(t)}{t-z}\,\mathrm{d}t = -\frac{\mathrm{i}+f}{2}\sum_{n=0}^{\infty} b_n R_{2n+1}(z) \tag{30}$$

[§]The approach described in Ref. 6 of expanding the function profile in terms of Chebyshev polynomials of the first kind $f(x) = \sum_{n=0}^{\infty} b_{2n}T_{2n}(x)$, may be equally used. However, we prefer to present this formulation as it allows a direct control of the representation of the closed-form contact law, and presents a more stable behaviour in the most challenging region for the convergence of the series, i.e. the region close to the contact area edges.

where $R_n(z) = [z - (z^2 - 1)^{1/2}]^n$. It is interesting to note that in the Hertzian case only the first term is non-zero, while in the case of the sharp wedge, an infinite number of terms is needed, and the convergence is slow and oscillatory, as this is the drawback of modelling the logarithmic singularity with continuous functions. Analytical results are possible for the coefficients in the latter case, as

$$b_n = \frac{4\theta}{\pi A} \frac{(-1)^{2n}}{2n+1}, \quad n = 0, 1 \ldots, \infty. \tag{31}$$

In the intermediate range, say, $a/b = 0.1$–1, the series is rapidly convergent. From the potential, the stresses, as well as the displacement derivatives, can be obtained from the standard relations [5, 6]

$$\frac{\sigma_x + \sigma_y}{2} = 2\mathrm{Re}\,\Phi(z), \tag{32}$$

$$\frac{\sigma_y - \sigma_x + 2i\tau_{xy}}{2} = (\bar{z} - z)\Phi'(z) - \bar{\Phi}(z) - \Phi(z) \tag{33}$$

The absolute displacements may be found only to within an arbitrary constant, which is a characteristic of plane elasticity. It is worth noting that $R_0(z) = 1$ for $n = 0$, and that the values on the $y = 0$ axis can be given in simpler form. In particular,

$$R_n(x) = \begin{cases} T_n(x), & |x| \leqslant 1, \\ [x - \mathrm{sgn}(x)(x^2 - 1)^{1/2}]^n & |x| > 1. \end{cases} \tag{34}$$

Also, on the y-axis, the expression simplifies to

$$R_n(y) = i[y - (y^2 + 1)^{1/2}]^n, \quad |y| \geqslant 0. \tag{35}$$

Therefore, in cases where values are needed only on the x or on the y-axis, these simplified equations may be used.

Some remarks on the details of the numerical computations are appropriate. First, a direct least-squares fitting approach has proved to be more efficient than the calculation of the Chebyshev coefficients from integral properties. The Fourier coefficients of this series have no physical interpretation, but the choice of a sufficiently large number of collocation points avoids the problem of oscillatory convergence which may arise in a direct calculation of the series coefficients, with the only minor drawback that, if the number of terms included is increased, all the coefficients have to be recalculated.

The partial slip cases are easily covered by means of superposition. In particular, the stress field can be obtained from the potential of the full sliding configuration, by adding the corrective stress field due to the perturbation shear $q^*(x)$, by means of a series in terms of Chebyshev polynomials

$$q^*(x) = -\sqrt{1 - x^2} \sum_{n=0}^{\infty} b_n^* U_{2n}(x). \tag{36}$$

Here x is normalized with respect to the dimension of the stick zone c. The corresponding corrective Muskhelishvili's potential is

$$\Phi_{\mathrm{corr}}(z) = -\frac{1}{2\pi i} \int_{-1}^{1} \frac{q^*(t)}{t - z}\, dt = -\frac{1}{2} \sum_{n=0}^{\infty} b_n^* R_{2n+1}(z). \tag{37}$$

Since the form of this stress field, on normalizing the coordinates, is *exactly* the same as the full sliding case, the partial slip case does not require *any* additional coding, except that relating to effecting superposition.

5. RESULTS

It is difficult to display comprehensive results for the complete state of stress over the neighbourhood of contact, even for sliding contacts, as there are two independent variables; the ratio of the extent of the "nose" to the size of the contact patch (a/b), and the coefficient of friction, f. The wedge angle θ enters the problem in a slightly unusual way; it is simply a multiplicative constant only in the

standard "sharp" wedge problem, but here it implicitly defines the radius of curvature, R, of the wedge apex, as continuity of slope is assumed at the transition point, and hence $\sin\theta = a/R$, or, for small θ, $R \approx a/\theta$; therefore θ is not an independent variable.

As it is the yield criterion that is of most interest in engineering applications for ductile materials and the maximum principal stress is needed for brittle materials, only results in terms of these two quantities will be shown. A Fortran library routine was used to calculate the maximum values of these parameters, for a single Poisson's ratio, i.e. $\nu = 0.3$, but for the complete range of ratio a/b from 0.1 to 1 in steps of 0.1, and friction coefficients in the range $f = 0, 0.8$ in steps of 0.0125. Von Mises' yield criterion was used, and transverse plane strain was assumed to arise.

5.1. *Normal loading*

Figure 3 shows plots of the normalized elastic limit $P/(bk)$, where k is the yield strength in pure shear, as a function of the ratio a/b. It may be seen that, compared with the Hertz limiting case $a/b = 1$, the strength here is always lower, as expected, since the pressure distribution here is more localized near the centre of the contact. The elastic limit in the sharp wedge case is theoretically zero, and it is worth remarking that in this case the state of stress implied at the apex of the indenter depends on the path along which it is approached. If we set $y = 0$ first, and approach along the surface, it is clear that $\sigma_{yy}(x, 0) = \sigma_{xx}(x, 0)$ and that they both tend to infinity as $|x| \to 0$. Yielding will therefore occur along the z axis. On the other hand, if x is set to zero first, so that the origin is approached along the axis of symmetry, the difference between the direct stresses remains finite at all depths, and is given by

$$|\sigma_{xx} - \sigma_{yy}| = \frac{4\theta a}{\pi A\sqrt{y^2 + a^2}}.$$

A major result of the present investigation is to that we have shown that for a ratio a/b as small as 0.1 the elastic limit is *still* $P/(bk) \simeq 3$, i.e. about half the limit for the optimal configuration (uniform pressure) [6] or about 60% of the Hertzian case. This clearly suggests that the simple Hertzian normal loading design, with a *safety factor* of 2, is appropriate even for a wedge indenter, provided that the dimension of the contact area is not larger than, say, 10 times the extent of the rounded part. If a more precise elastic limit is required the data given in Fig. 3 are appropriate. Also shown in the figure is the depth, y_m, at which first yield occurs. This is at $y_m/b = 0.7$, the Hertzian case, when $b/a \leqslant 1$, and moves up to the surface, $y_m/b = 0$, as $a/b \to 0$, i.e. the sharp wedge geometry is approached.

5.2. *Full sliding case*

We turn now to the case where a tangential load, sufficient to cause sliding, has been applied. Figure 4 shows the dependence of the elastic limit $P/(bk)$ on the friction coefficient f. First, it is clear that, starting from the Hertzian configuration $a/b = 1$, it is well known [6] that, for small coefficients of friction, less than about $f = 0.3$ the severest state of stress remains subsurface, whilst for higher

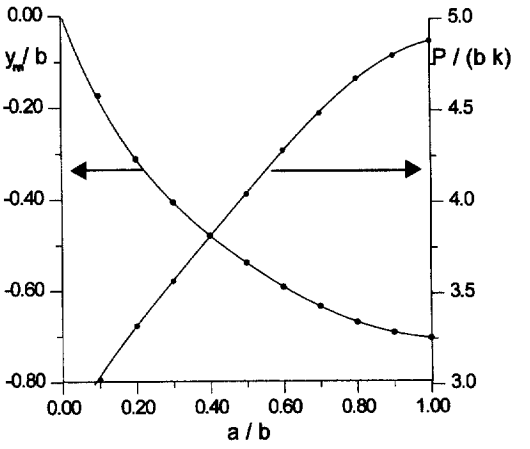

Fig. 3. Elastic limit $P/(bk)$ for a normal indentation, and vertical location of the yield point, as function of the ratio a/b. Poisson's ratio $\nu = 0.3$.

values of f the tendency to yield is greatest on the surface. This response gives rise to the cusp of the upper curve in Fig. 4. When a rounded wedge case is considered, the yield point tends to move to the origin with an increase in contact dimension, b/a, as discussed above; with an increase in the coefficient of the friction this migration to the surface occurs more rapidly. In the limiting sharp wedge case, it is clear that the vertex is always a singular point.

It is worth noting that, as the friction coefficient is increased, the difference between the Hertzian and rounded wedge configuration as measured by a yield parameter tends to *decrease*, as the severest state of stress arises on the edge of the contact area, and is less dependent on the precise distribution of the normal and shearing tractions.

The effect of the frictional traction is displayed in an alternative form in Fig. 5, where the point of maximum von Mises yield parameter is identified in detail. Starting from the normal loading case ($f = 0$), the point moves from the axis of symmetry, towards the trailing edge of the contact, as it migrates towards the surface; each little cross corresponds to an increment of the friction coefficient of 0.0125. When f has reached a particular value (that can be obtained also from the cusp points in Fig. 4), the maximum jumps to the surface, is the sense that the local maximum on the surface suddenly becomes the global maximum. As can be seen from Fig. 4, when the strength of the contact is surface-controlled the severity of the state of stress increases rapidly with f, and hence the contact strength falls abruptly. In fact, when the strength of the contact is controlled by a subsurface point it is only weakly dependent on the coefficient of friction, particularly when the radius of the nose is

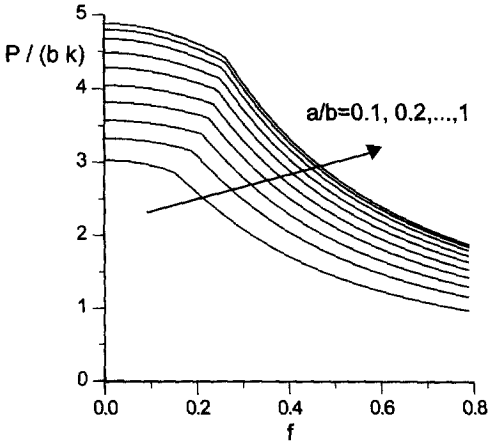

Fig. 4. Elastic limit $P/(bk)$ in the full sliding configuration, as a function of the friction coefficient f, for different values of the ratio a/b, in the range $a/b = 0.1, 0.2, \ldots, 1.0$. Poisson's ratio $\nu = 0.3$.

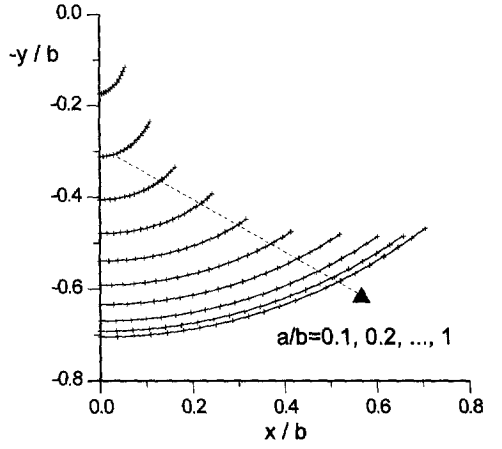

Fig. 5. Location of the yield point in the (lower) half-pane, for different values of the ratio a/b; note that each cross correspond of a increment on the friction coefficient of 0.0125, and that only subsurface values are displayed. The point where the maximum jumps from the subsurface to the surface corresponds to the cusp points in Fig. 4. Poisson's ratio $\nu = 0.3$.

small ($b \gg a$), but the critical value of f is also smaller for $b \gg a$. Therefore, from the point of view of the design of styli, there is a great deal to be said for attempting to maintain the coefficient of friction below the critical value, perhaps by lubrication.

Also of importance is the maximum tension induced at the surface, as this is the quantity which is responsible for initiating surface defects and their initial propulsion as cracks. The point of maximum tension lies at the trailing edge of the contact patch, for Hertzian, sharp wedge and rounded wedge cases. The relevant values are

$$a\frac{\sigma_1^{\max}}{fP} = \begin{cases} 1, & \text{shape wedge case} \\ 4/\pi, & \text{Hertzian case,} \end{cases} \tag{38}$$

and for intermediate cases no simple closed-form exists, but it is clear that the Hertzian result provides a safe upper bound for design purposes. It is worth emphasizing that the presence of the apex actually *decreases* the concentration of tension: this is apparent from a consideration of the distribution of shear, which is solely responsible for this tension, as it is less localized at the trailing edge, and the variation is only 21% of the original Hertzian value. The transition from the 'sharp' solution to the Hertzian is displayed in Fig. 6.

5.3. *Partial slip case*

Figure 7 shows some traction distributions arising for some particular cases of partial slip regime. The case shown is $a/b = 0.25$, and 3 different values of the tangential load are considered, for which

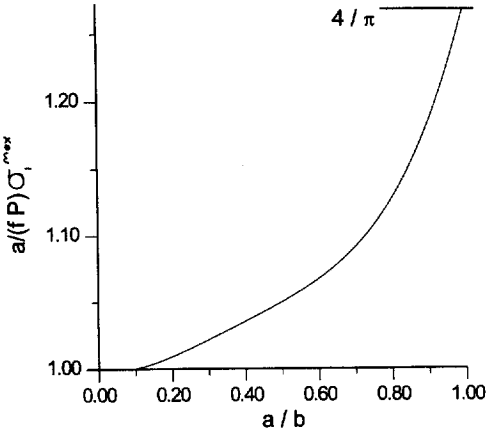

Fig. 6. Values of the non-dimensionalized maximum principal stress $(a/fP)\sigma_1^{\max}$ at the trailing edge of the full sliding contact, as a function of the ratio a/b.

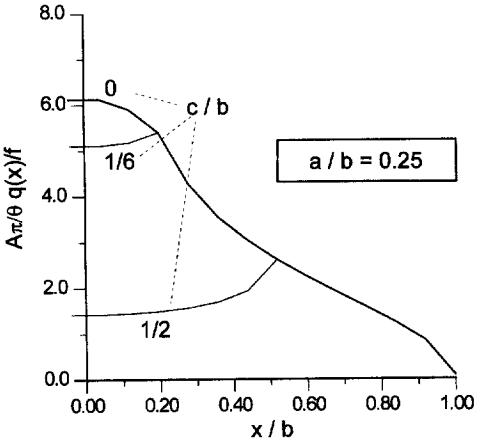

Fig. 7. Non-dimensionalized shearing tractions $-q(x/b)\ A\pi/f\theta$ in the partial slip regimes. The contact geometry is fixed to $a/b = 0.25$, and 3 different values of the tangential load are considered, for which $c/b = 0, 1/6, 1/2$, corresponding, respectively, to full sliding contact, Cattaneo–Mindlin corrective solution, and edge of stick zone lying in the linear part of the profile.

$c/b = 0, 1/6, 1/2$, respectively when the contact is full sliding, the stick zone lies only in the rounded part (Cattaneo–Mindlin corrective solution), and stick zone lying in the linear part of the profile too.

Regarding the strength of such contacts, the number of parameters become impractically large [a/b, f, $Q/(fP)$], and therefore it is not possible to cover all possible regimes. However, since the corrective shear distribution always reduces the local value of the shearing traction, and since they are the principal quantities controlling yield, it is *likely* that the elastic limit for the full sliding can be considered an upper bound for strength, therefore allowing a *safe* design. Also, it is believed that a more refined design procedure is not warranted, as the partial slip regime is likely to occur between vibrating components, where the coefficient of interfacial friction and magnitude of applied shear are not known within precise limits. Also, in these cases a more refined approach using the framework of Linear Elastic Fracture Mechanics is usually required.

6. CONCLUSIONS

The indentation by a wedge punch with rounded tip has been studied. Normal loading, as well as full sliding and partial slip regimes have been treated and solutions in either a closed form or as a rapidly convergent series have been found. The transition from Hertzian to a sharp wedge punch has been fully studied. One of the most noteworthy and unexpected results is that the strength of the contact is about 60% of the equivalent Hertzian case for an extent of the rounded part as small as about 1/10 of the contact dimension. It follows that for many wedge-type indentation processes the presence of even a modest finite radius at the apex of the indenter has a profound influence of the strength of the contact, and the strength of the contact immediately becomes quantifiable. This will be true whether or not the results found are applied to macroscopic indenters, or the kind of nano-indenter currently being employed where the tip radius may well be specified in terms of a number of atomic diameters.

REFERENCES

1. Truman, C. E., Sackfield, A. and Hills, D. A., Contact mechanics of wedge and cone indenters. *International Journal of Mechanical Sciences*, 1995, **37**(3), 261–275.
2. Yoshimoto, G. and Tzukizoe, T., On the mechanism of wear between metal surfaces. *Wear*, 1958, **1**, 472.
3. Hills, D. A. and Nowell, D., The development of a fretting fatigue experiment with well-defined characteristics. In *Standardization of Fretting Fatigue Test Methods and Equipment*. ASTM STP 1159, eds. M. H. Attia and R. B. Waterhouse. ASTM, Baltimore, 1992, pp. 69–84.
4. Shtayerman, I. Ya., *Contact Problems of the Theory of Elasticity*. Leningard, Moscow. Gostekhteoretizdat, 1949. Available from the British Library in a English translation by Foreign Technology Div., FTD-MT-24-61-70, 1970.
5. Muskhelishvili, N. I., *Singular Integral Equations*, Noordhoff International Publishing, 1977 (Translated by J. R. M. Radok).
6. Hills, D. A., Nowell, D. and Sackfield, A., *Mechanics of Elastic Contacts*. Butterworth, Heinemann, 1993.
7. Sackfield, A. and Hills, D. A., Sliding contact between dissimilar elastic bodies. *J. Tribology*, **110**(4), 592–596.

APPENDIX: DERIVATION OF THE PRESSURE DISTRIBUTION

To integrate Eqn (3), we made use of an integral calculated by Shtayerman [4] for the similar case of a flat punch with rounded edges. Considering that the function $h'(t)$ is described by Eqn (6), one has

$$p(x) = \frac{\theta/a}{\pi A}\sqrt{b^2 - x^3}\left[\int_{-b}^{-a}\frac{a\,dt}{\sqrt{b^2 - t^2}(t - x)} - \int_{-a}^{a}\frac{t\,dt}{\sqrt{b^2 - t^2}(t - x)} - \int_{a}^{b}\frac{a\,dt}{\sqrt{b^2 - t^2}(t - x)}\right]. \tag{A1}$$

Now, define $\varphi_0 = \arcsin a/b$, $t = 2\tau b/(1 + \tau^2)$, and $x = 2\xi b/(1 + \xi^2)$; we find

$$\int_{x_1}^{x_2}\frac{dt}{\sqrt{b^2 - t^2}(t - x)} = \frac{1 + \xi^2}{b}\int_{\xi_1}^{\xi_2}\frac{d\tau}{(\tau - \xi)(1 - \tau\xi)} \tag{A2}$$

$$= \frac{1 + \xi^2}{b(1 - \xi^2)}\left[\int_{\xi_1}^{\xi_2}\frac{d\tau}{(\tau - \xi)} - \int_{\xi_1}^{\xi_2}\frac{d\tau}{(\tau - 1/\xi)}\right], \tag{A3}$$

where ξ_1, ξ_2 are related to x_1, x_2 by

$$x_1 = \frac{2\xi_1}{1 + \xi_1^2}b, \quad x_2 = \frac{2\xi_2}{1 + \xi_2^2}b. \tag{A4}$$

Considering that the integrals must be intended as CPV, and assuming $\xi = \tan\varphi/2$ and $a = b\sin\varphi_0$, it follows that $x = b\sin\varphi$, and

$$\int_{-b}^{-a} \frac{a\,dt}{\sqrt{b^2-t^2}(t-x)} - \int_{a}^{b} \frac{a\,dt}{\sqrt{b^2-t^2}(t-x)} = \frac{a}{b\cos\varphi} \ln\left|\frac{\sin(\varphi+\varphi_0)/2}{\cos(\varphi-\varphi_0)/2}\right| \Big/ \left|\frac{\cos(\varphi+\varphi_0)/2}{\sin(\varphi-\varphi_0)/2}\right|. \tag{A5}$$

Moreover, with the same procedure

$$\begin{aligned}\int_{-a}^{a} \frac{t\,dt}{\sqrt{b^2-t^2}(t-x)} &= \int_{-a}^{a} \frac{dt}{\sqrt{b^2-t^2}} + x\int_{-a}^{a} \frac{dt}{\sqrt{b^2-t^2}(t-x)} \\ &= 2\varphi_0 + \frac{x}{b\cos\varphi} \ln\left|\frac{\sin(\varphi-\varphi_0)}{\sin(\varphi+\varphi_0)}\right|,\end{aligned} \tag{A6}$$

where the first integral is elementary using the substitution $t = b\sin\varphi$. Substituting the integrals into the expression for the pressure $p(x)$,

$$\frac{\pi A}{\theta}\,p(x) = \ln\left|\tan\frac{\varphi+\varphi_0}{2}\tan\frac{\varphi-\varphi_0}{2}\right| - 2\varphi_0\frac{\cos\varphi}{\sin\varphi_0} - \frac{\sin\varphi}{\sin\varphi_0}\ln\left|\frac{\sin(\varphi-\varphi_0)}{\sin(\varphi+\varphi_0)}\right|, \tag{A7}$$

Regarding the equilibrium condition (5), assuming $t = b\sin\varphi$,

$$\begin{aligned}-\frac{AP}{\theta} &= \int_{-b}^{-a} \frac{t\,dt}{\sqrt{b^2-t^2}} - \frac{1}{a}\int_{-a}^{a} \frac{t^2\,dt}{\sqrt{b^2-t^2}} - \int_{a}^{b} \frac{t\,dt}{\sqrt{b^2-t^2}} \\ &= -2b\cos\varphi_0 + \frac{b^2}{a}\left(\frac{\sin 2\varphi_0}{2} - \varphi_0\right) = -\frac{a}{\sin^2\varphi_0}\left(\frac{\sin 2\varphi_0}{2} + \varphi_0\right).\end{aligned} \tag{A8}$$